ACS OMEGA

http://pubs.acs.org/journal/acsodf

Article

Application of Novel Colloidal Silica Nanoparticles in the Reduction of Adsorption of Surfactant and Improvement of Oil Recovery Using Surfactant Polymer Flooding

Himanshu Kesarwani, Shivanjali Sharma,* and Ajay Mandal*

Cite This: *ACS Omega* 2021, 6, 11327−11339

Read Online

ACCESS | Metrics & More | Article Recommendations

ABSTRACT: Surfactant polymer flooding is one of the most common chemical enhanced oil recovery techniques, which improves not only the microscopic displacement of the fluid through the formation of the emulsion but also the volumetric sweep efficiency of the fluid by altering the viscosity of the displacing fluid. However, one constraint of surfactant flooding is the loss of the surfactant by adsorption onto the reservoir rock surface. Hence, in this study, an attempt has been made to reduce the adsorption of the surfactant on the rock surface using novel colloidal silica nanoparticles (CSNs). CSNs were used as an additive to improve the performance of the conventional surfactant polymer flooding. The reduction in adsorption was observed in both the presence and absence of a polymer. The presence of a polymer also reduced the adsorption of the surfactant. Addition of 25 vol % CSNs effectively reduced the adsorption of up to 61% in the absence of a polymer, which increased to 64% upon the introduction of 1000 ppm polymer in the solution at 2500 ppm of the surfactant concentration at 25 °C. The adsorption of surfactant was also monitored with time, and it was found to be increasing with respect to time. The adsorption of surfactant increased from 1.292 mg/g after 0.5 days to 4.179 mg/g after 4 days at 2500 ppm of surfactant concentration at 25 °C. The viscosity, surface tension, and wettability studies were also conducted on the chemical slug used for flooding. The addition of CSNs effectively reduced the surface tension as well as shifted the wettability toward water-wet at 25 °C. Sand pack flooding experiments were performed at 60 °C to access the potential of CSNs in oil recovery, and it was found that the addition of 25 vol % CSNs in the conventional surfactant polymer chemical slug aided in the additional oil recovery up to 5% as compared to that of the conventional surfactant polymer slug.

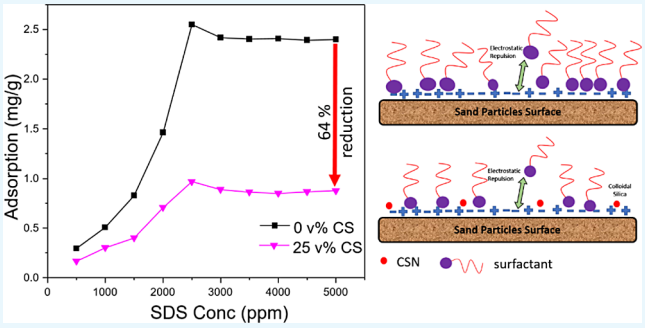

1. INTRODUCTION

The demand for oil is increasing day by day and is expected to only increase in the near future. No new big discovery is forcing the mature fields to produce more from the residual oil (after primary recovery), which is approximately 70% of the total oil in place, which is the target for the enhanced oil recovery (EOR).[1−5] In recent years, a lot of researchers have tried to contribute to the field of EOR.[6−9] Surfactant polymer flooding is a chemical EOR process, which is one of the most promising ways of exploiting the remaining oil from the reservoir. Since surfactant polymer flooding involves both macroscopic and microscopic displacement of fluids, it provides better oil recovery as compared to conventional surfactant flooding, which focuses only on the microscopic displacement of fluid.[10−12] The only big hurdle in implementing surfactant polymer flooding is the adsorption of the surfactant on the rock surfaces. The addition of polymer to the conventional surfactant flooding not only reduces the adsorption of the surfactant up to some extent,[13] but it also helps in increasing the macroscopic displacement efficiency of the chemical slug by increasing the viscosity of the displacing fluid.[14,15] The addition of polymer increases the rheological parameter of the chemical slug as well as reduces the viscous fingering of more mobile phases.[2,16] The increase in the viscosity of the displacing fluid results in controlling the mobility ratio,[17] which is one of the most important parameters in the case of calculating the macroscopic displacement efficiency.[10,18]

Adsorption is a surface phenomenon that reduces the activity of surfactants. The surfactant molecules get adsorbed on the rock surface; therefore, the surfactant activity decreases,

Received: January 17, 2021
Accepted: April 14, 2021
Published: April 19, 2021

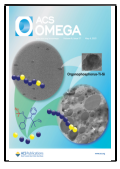

which is one of the major challenges with surfactant flooding. Several additives, such as alkali and polymers, have been used by the researchers to reduce the adsorption of the surfactant on the rock surface. Seethepalli et al.[19] have reported that the surfactant adsorption can be reduced by the addition of alkali. Saxena et al.[20] have performed an experimental investigation on the role of minerals, alkalinity, salinity, and nanoparticles on the adsorption of the surfactant and have reported that the silica nanoparticles were more efficient in reducing the surfactant adsorption when compared with alkali. However, Wang et al.[21] have reported the reduction in the adsorption of the surfactant when a preflush of polymer slug was injected. The adsorption reduction could be attributed to the formation of a polymer layer on the rock surface that resists the adsorption of surfactant molecules and thereby reduces the adsorption of the surfactant on the rock surface.

The application of nanoparticles in the petroleum industry is not new.[1,22−25] Researchers are continuously trying to modify even surfactant polymer flooding by the addition of nanoparticles in the chemical slug that could reduce the adsorption of the surfactant as well as the interfacial tension (IFT), which could lead to the recovery of more oil from mature fields.[6,26−28] Nanoparticles are of great interest to scientists because of their small size and larger surface area. A lot of researchers have published their work in the field of oil and gas industry using nanoparticles.[29−31] Cheraghian and Hendraningrat[32] have done a review on the application of nanoparticles in the field of EOR. Researchers have used nanoparticles for the reduction of IFT and the stabilization of pickering emulsion of crude oil and water that helps in recovering more oil from the reservoir. Nanoparticles have also been used to reduce the adsorption of the surfactant on the rock surfaces.[29,33] Ahmadi and Sheng[33] have used hydrophilic and hydrophobic silica nanoparticles for the reduction of adsorption of the surfactant on the carbonate rock surface. They have reported that the silica nanoparticles have effectively reduced the surfactant adsorption on the rock surface by approximately 45%. The reason for the reduction in adsorption could be the hydrogen bonding between the negatively charged head of the surfactant and the hydrogen present in the hydroxyl group of silica in the aqueous form.[20,34] Wu et al.[29] have also studied the effect of silica nanoparticles on the reduction of adsorption on the sand particle surface. They have also reported the reduction of adsorption by approximately 40%. The reduction in adsorption could be attributed to the accumulation of silica nanoparticles on the sand particle wall, resulting in reducing the adsorption area available for the surfactant. Ahmadi and group[35−37] have used silica nanoparticles on both sandstone and carbonate rock samples and have reported the reduction in the adsorption of the surfactant as well as increased oil recovery. The reduction in adsorption as well as the reduction in the IFT makes them a preferential choice for the design of chemical slug for EOR.

Based on the previous literature available, it can be concluded that the nanoparticles can be used for the surfactant adsorption reduction and EOR, but the main challenge faced is the dispersion of the powdered nanoparticles in the aqueous solution. To encounter this, we have used colloidal silica nanoparticles (CSNs) in the present study, which are a stable dispersion of silica nanoparticles that are in the range of 1−100nm. CSNs are in the liquid state, whereas the fumed or precipitated silica is in a powdered form. Conventional silica nanoparticles that are in the powdered form tend to form aggregates in the solution, resulting in a higher particle size, and subsequently settles down. However, CSNs, unlike amorphous silica, do not agglomerate and remain in smaller sizes even after many days. CSNs are in a dispersed form; hence, mixing of nanoparticles is easier as compared to powdered silica nanoparticles. Being in small size, they possess all their benefits and have an edge in the performance when compared with the powdered silica nanoparticles. Also, they differ in their composition; the sodium silicates have a SiO_2/Na_2O ratio of ∼3.5, whereas the same for CSNs is >50. Apart from these, CSNs have viscosity values comparable to those of water. The difference in the properties and composition of CSNs makes them a novel additive for the investigation of their applicability in the field of EOR. The application of the CSNs for the performance improvement of the surfactant polymer flooding has been done for the first time to the best of our knowledge. The presence of the CSNs in the aqueous phase could result in the interaction between the hydrophilic negatively charged head of the surfactant with the hydrogen present in the hydroxyl group of the nanoparticles through the hydrogen bonds. This could result in keeping the surfactant molecules in the bulk phase, which in turn could reduce the adsorption of the surfactant.

In this work, an attempt to reduce the adsorption of an anionic surfactant on the sand particles has been made using the CSNs. The effect of the concentration of CSNs on the adsorption of sodium dodecyl sulfate (SDS) was investigated in both the presence and the absence of polymer. The adsorption of the surfactant on the sand particle surface with respect to time was also monitored. Surface tension and contact angle studies were performed in the presence and absence of CSNs to check its effect on the interfacial property and applicability in the field of EOR. Next, the viscosity of the chemical slug prepared was also analyzed over a wide range of shear rates. Finally, the effect of CSNs on the oil recovery was investigated by performing the sand pack flooding experiments, which were compared with the conventional surfactant polymer flooding.

2. EXPERIMENTAL SECTION

2.1. Materials. CSNs (CC401) in the dispersion form, of particle size 12 nm, were procured from Nouryon, Mumbai. Sodium lauryl sulfate commonly known as SDS of purity >93% was procured from Rankem Chemicals. Common industrial polymer polyacrylamide (PAM) was procured from SNF Floerger, France. Crude oil used in the flooding experiments with a viscosity of 6.22 cP at 60 °C and an acid number of 1.12 mg KOH/g was obtained from Ankleshwar Field, ONGC. Toluene having a purity of >99% used in the flooding experiments was procured from SD-Fine Chemicals. Sodium chloride (NaCl) of purity >99.9% was procured from Sisco Research Laboratories Pvt. Ltd. Normal beach sand (400−500 μm) was used in the experiment after washing it with deionized water and drying at 105 °C in an hot air oven overnight to remove any moisture.

2.2. Critical Micelle Concentration Determination. The critical micelle concentration (CMC) of the surfactant was determined using the conductivity measurement of the surfactant solution of varying concentrations. Conductivity is the dissociation of the ions in the aqueous phase. The conductivity of the anionic surfactant solution increases with an increase in the surfactant concentration up to its CMC value, after which the slope of the conductivity versus

https://doi.org/10.1021/acsomega.1c00296
ACS Omega 2021, 6, 11327−11339

surfactant concentration decreases due to the formation of the micelles.[27,38] The surfactant solution of varying concentrations from 500 to 5000 ppm in the interval of 500 ppm was prepared in deionized water using a magnetic stirrer at 800 rpm for approximately 1 h. A LABMAN Multiparameter LMMP-30 (LABMAN Scientific Instruments) was used for the measurement of the conductivity of the samples. The equipment was first calibrated using the standard solution provided by the manufacturer, followed by the measurement of the conductivity of the surfactant solution. The probe of the equipment was washed gently using deionized water after each measurement. Then, the probe was gently wiped using the Kimwipes tissue paper. Further, deionized water was used to measure the conductivity to make sure no surfactant was adsorbed on the probe, followed by the measurement of the conductivity of the next surfactant solution. The experiments were performed at 25 °C.

2.3. Adsorption Experiments. The methodology to evaluate the adsorption of the surfactant on the rock surface was kept the same as that performed by the previous scholars.[33,39] Surfactant solutions (10 mL) were prepared with varying concentrations of the surfactant from 500 to 5000 ppm. The conductivity of each solution was measured carefully using a conductivity meter. Sand particles (1 g) of 400 μm were added to the solution, and the solution was kept undisturbed for 24 h. After 24 h, the sand particles were separated from the surfactant solution using a centrifuge, and the conductivity of each sample was measured again. A standard curve of conductivity with varying concentrations of the surfactant was drawn, which was used later as a reference to determine the concentration of the surfactant remaining in the aqueous phase after the sand particles were separated. The difference between the initial and final concentration of the surfactant was measured. To measure the amount of surfactant concentration reduced in the 500 ppm surfactant concentration solution, the conductivity of 250 ppm surfactant solution was measured. The measurement was performed at 25 °C and 14.7 psi, and the ratio of the mass of the sand particles added to the surfactant solution to the volume of the surfactant solution was kept the same in all the cases. The surfactant molecules adsorbed on the sand particles were separated from the solution by the centrifuge, and the decrease in the surfactant concentration in the solution gives the adsorbed quantity of the surfactant on the sand particles. The adsorption was calculated using eq 1.[33,40]

$$A = \frac{\left[(C_i - C_f) \times \frac{M_s}{M_r}\right]}{1000} \quad (1)$$

where A is the adsorption of the surfactant in mg/g; C_i and C_f are the initial and final concentrations of the surfactant, respectively, in solution in ppm, M_s is the mass of the solution in grams, and M_r is the mass of the rock samples added to the surfactant solution in grams.

2.3.1. Adsorption of the Surfactant in the Presence of CSNs. Four different sets of surfactant solutions of varying concentrations were prepared with 0, 5, 15, and 25 vol % of CSNs. The conductivity of the solutions was measured before the addition of sand particles as well as after the removal of sand particles, which was used to find out the difference in the concentration of the surfactant. Equation1 was used to calculate the adsorption of surfactants in the presence of CSNs.

2.3.2. Adsorption of Surfactant in the Presence of Polymer and CSNs. The samples were prepared with varying concentrations of the surfactant and CSNs, whereas a fixed amount of PAM (1000 ppm) was added to each solution. The process of the conductivity measurement was kept the same, and eq 1 was used to calculate the quantity of the surfactant adsorbed on the sand particle surface in the presence of polymer and nanoparticles.

2.3.3. Effect of Time on Surfactant Adsorption. The surfactant solutions with varying concentrations of the surfactant were prepared, and their conductivity with the variation of time was measured. A standard curve of conductivity versus concentration was plotted, which was used to evaluate the concentration of the surfactant remained in the solution after the sand particles were separated using centrifugation. The surfactant adsorption was measured after 0.5, 1, 2, 3, and 4 days.

2.4. Surface Tension and Contact Angle Measurements. To establish any change in the wetting characteristics of the fluid on the rock surface, surface tension and dynamic contact angle studies were performed using a syringe pump (D-CAM Engineering, India), a high-speed camera (Phantom Tech VEO 640L), and an evacuated chamber. Initially, the syringe pump was filled with the liquid under study and injected at a flow rate (0.001 mL/min) to a surface kept in an evacuated chamber. Upon exiting the needle, the liquid emerged as a pendant drop, which was captured at the moment it detached from the needle. The liquid formed a sessile drop as it touched the surface, which was captured at regular intervals using a high-speed camera. The surface used for the contact angle measurement was an oil-wet glass slide. The glass slide was dipped in the crude oil for 7 days to ensure oil-wetting characteristics. All the measurements were taken at 25 °C and 14.7 psi. The flow lines were cleaned by flowing the deionized water through it twice, and the image of deionized water was checked to ensure that no traces of impurity were present in the flow lines. The images obtained were analyzed using the ImageJ software.

2.5. Viscosity Measurements. The viscosity measurements were made using the Anton Paar rheometer (MCR-52). The viscosity of the slug was measured to understand the effect of the shear rate on the viscosity of the chemical slug. A stainless steel double gap pressure cell geometry from Anton Paar (DG35.12) was used for viscosity measurements. The outer diameter of the cup was 32.000 mm, while the length of the bob was 60.000 mm. The outer and inner diameters of the bob were 35.120 and 32.800 mm, respectively. The system was not pressurized during the experiments. To understand the shear-dependent properties of the fluid, the shear rate was varied from 1 to 1000 s^{-1}. The measurements were made at 30, 60, and 90 °C. The equilibrium time of 3 min, after the temperature reached the desired value, was given for the samples, after which the viscosity was measured. The variation of the viscosity against the shear rate could provide an understanding about the behavior of the chemical slug and also its deformation concerning shear rate and temperature. All the parts of the equipment were carefully washed with deionized water and dried before and after each measurement.

2.6. Dynamic Light Scattering Analysis. Dynamic light scattering (DLS) experiments were performed to investigate the particle size distribution of the CSNs. A Malvern Zetasizer Nano-ZS instrument was used for the measurement of the average hydrodynamic diameter and the zeta potential

https://doi.org/10.1021/acsomega.1c00296
ACS Omega 2021, 6, 11327−11339

measurement of the nanoparticles dispersed in the water. A small volume of the batch CSNs (~1.5 mL) was poured into the cuvette, which was used for the measurement of the particles size. The DLS experiments were performed at 30 °C. A standard laser beam of a wavelength of 633 nm is passed through the samples, which measures the particle diffusion in Brownian motion dispersed in the liquid phase and uses the Stokes−Einstein equation to obtain the particle size. The cuvette was cleaned with methanol twice to remove any impurities present in it, and the equilibrium time of 120 s was set in the instrument to equilibrate the temperature for the measurement.

2.7. Flooding Experiments. Sand pack flooding was used to evaluate the effect of CSNs on the oil recovery that could be obtained by the surfactant polymer flooding. A sand pack of 30 cm in length and 2.54 cm in diameter was used for the flooding experiments with normal beach sand particles of 400−500 μm.[41] The schematic of the equipment is given in Figure 1. A

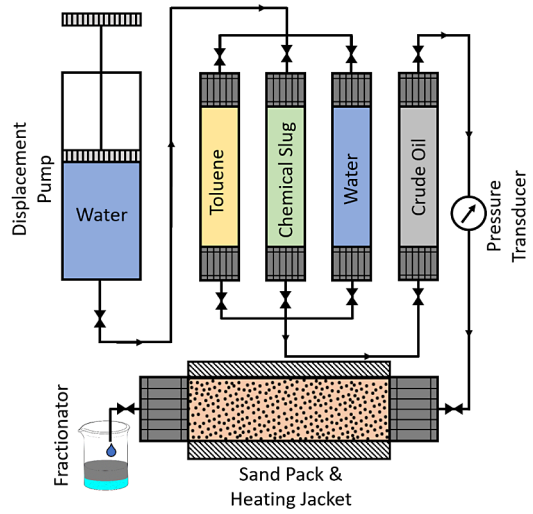

Figure 1. Schematic of the flooding apparatus used in the experiment.

sand pack was prepared by ramming the sand particles into the sand pack holder. A measured volume of 1 wt % brine (1 wt % NaCl) was taken in a wash bottle, which was used during the sand pack preparation. The volume of brine remaining in the wash bottle was subtracted from its original volume to find out the volume of the brine that was absorbed in the pore spaces of the sand pack. A constant flooding rate of 1 mL/min was maintained for all the flooding using a syringe pump capable of providing 10 000 psi, manufactured by the D-CAM Engineering, Ahmedabad. The sand pack was first flooded with 1 wt % brine to evaluate the porosity and permeability of water. Oil was then flooded to the sand pack to evaluate the initial oil saturation, which was again displaced with water to simulate the water flooding in the reservoir. After oil flooding, the flow lines were cleaned by flowing toluene through it. Initial oil saturation was obtained by the volume of water displaced by the oil when the oil was flooded into the sand pack. After water flooding, a chemical slug of 0.5 pore volume (PV) was injected into the sand pack, which would displace the amount of oil left after the secondary recovery. After the injection of chemical slug, chase water was flooded into the sand pack till the water cut reached 100% to ensure no further oil could be recovered from the sand pack. The flooding experiments were performed at 60 °C. Four chemical slugs were prepared containing 1000 ppm of polymer and 2500 ppm of surfactant and CSNs of varying concentrations of 0, 5, 15, and 25 vol %. In total, 0.5 PV of this solution was used as a chemical slug, which was injected into the sand pack followed by flooding of chase water.

3. RESULTS AND DISCUSSION

In this section, the effect of CSN concentration on the CMC of the surfactant has been reported. This is followed by the adsorption studies of the surfactant and the effect of the CSNs as well as the polymer concentration on the adsorption of surfactant on the sand particles. The adsorption of surfactant with respect to time was also investigated. Next, the effect of CSNs on the surface tension as well as on the wettability alteration has also been reported, followed by which the effect of nanoparticles on the viscosity of the chemical slug has also been reported. Finally, the application of CSNs in the EOR has been investigated through the sand pack flooding.

3.1. CMC Measurements. The CMC gives the minimum concentration limit of the surfactant above which surfactants began to form micelles. The conductivity of the surfactant was measured to obtain the CMC.[38] Conductivity is due to the presence of the surfactant ions in the aqueous solution. The conductivity of the surfactant increases with an increase in surfactant concentration, which is due to the increase in the number of the ions in the aqueous phase. As the surfactant reached its CMC value, the slope of the conductivity versus concentration graph decreases (Figure 2), which is due to the

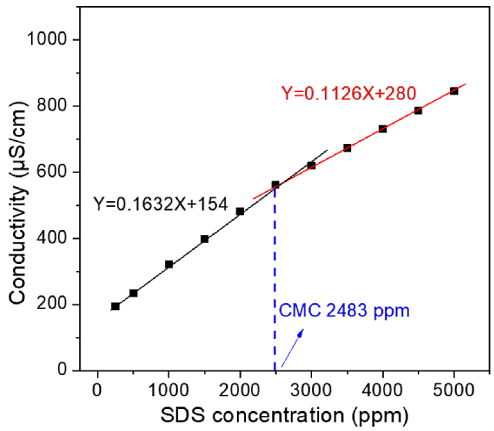

Figure 2. CMC measurement of SDS through conductivity measurement.

formation of micelles.[33] Since the conductivity of the surfactant is only due to the free surfactant ions present in the aqueous phase, when the surfactant concentration increases beyond its CMC value, the surfactant molecules begin to form micelles and the ratio of free surfactant molecules to surfactant micelles decreases; hence, the slope of the conductivity graph decreases. The sharp change in the nature of the curve was obtained at 2483 ppm (8.61 mM/L), which was reported as the CMC of the surfactant. The CMCs of the SDS in the previous study were found to be 8.2 and 9.54 mM/L.[42,43]

3.2. Surfactant Adsorption in the Absence of Polymer. Adsorption, being of critical importance in the case of surfactant flooding, was found to be reduced with an increase in the CSN concentration (Figure 3a). Different concentrations of CSNs (5, 15, and 25 v/v) were taken in the surfactant solution to understand their effect on the adsorption

https://doi.org/10.1021/acsomega.1c00296
ACS Omega 2021, 6, 11327−11339

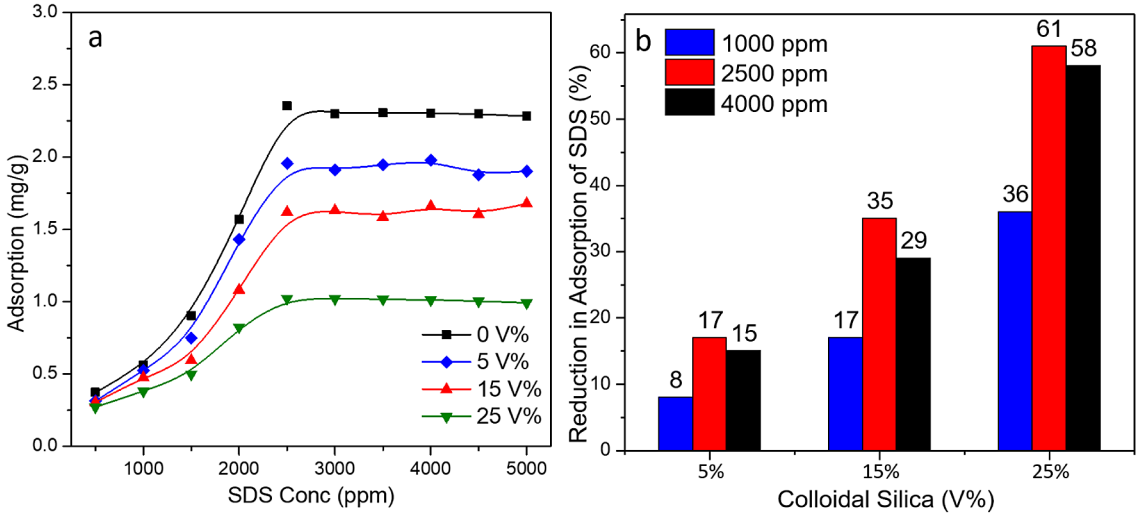

Figure 3. Adsorption of SDS in the absence of polymer: (a) effect of CSN concentration and the (b) effect of surfactant concentration on the percentage reduction of adsorption.

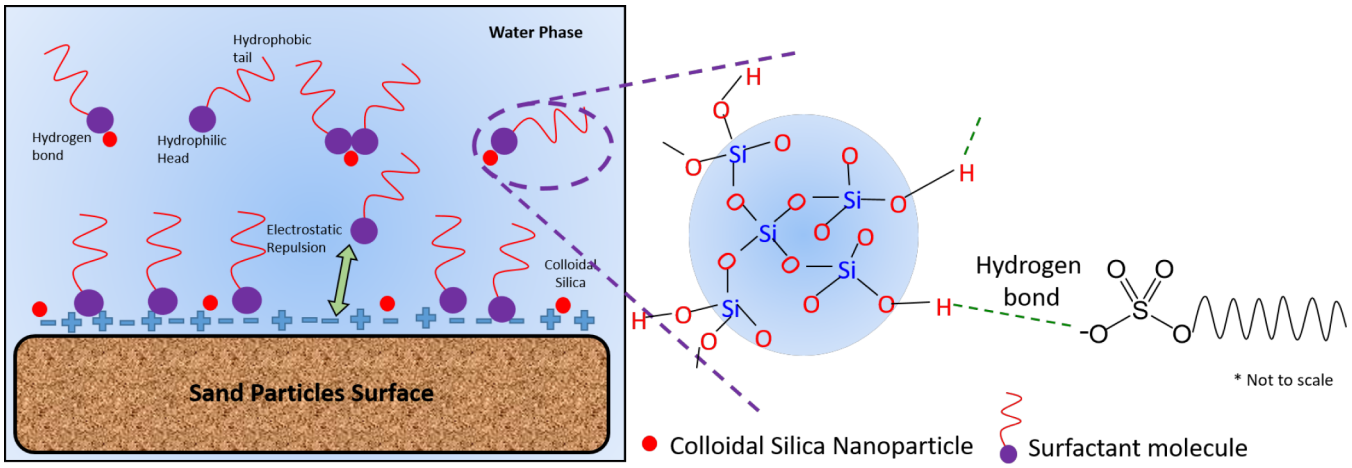

Figure 4. Adsorption of SDS on the sand particle surface in the presence of CSNs.

of the SDS on the sand particle surface. Surfactant adsorption was found to be 0.374 mg/g corresponding to the 500 ppm of SDS, which was found to be increasing with an increase in the SDS concentration and reaches up to a maximum value of 2.606 mg/g at 2500 ppm of SDS. This was reduced from 0.374 to 0.256 mg/g at 500 ppm of SDS with the variation of CSN concentration in the aqueous solution of the surfactant. As the concentration of the SDS was increased beyond 2500 ppm, no further increment in the adsorption value was found; instead, it remains constant. When the SDS concentration was below 2500 ppm, the molecules of SDS were free and readily got adsorbed as they are negatively charged and the sand particle (coarse) surface is positively charged.[44] Hence, the adsorption increased with an increase in the surfactant concentration up to 2500 ppm. As the concentration of the surfactant was increased beyond 2500 ppm, the free molecules of the surfactant began to form micelles among other surfactant molecules and did not get adsorbed on the sand particles, which explains no significant change in the value of the adsorption of SDS beyond 2500 ppm. This states that adsorption is only affected by the free molecules of the surfactant present in the aqueous phase.

As the CSNs were introduced in the aqueous solution of the surfactant, the hydrophilic head of the surfactant got attracted toward the hydroxyl group of the nanoparticles by a hydrogen bond. Therefore, it reduced the number of the free molecules of the SDS present in the aqueous solution and, hence, reduced the adsorption of SDS on the sand particles. Figure 3b illustrates the effect of SDS concentration on the reduction of its adsorption in the presence of CSNs. It was found that the reduction in the adsorption of the surfactant kept increasing till 2500 ppm, beyond which the change was not significant. This could be explained by the number of free molecules of SDS present in the solution, which kept increasing till 2500 ppm, giving rise to the adsorption of the surfactant, and began to form micelles beyond 2500 ppm, thus did not affect the adsorption significantly. As the CSN concentration of the solution increased from 5 to 25 vol %, the reduction in adsorption increased from 17% to 61% at 2500 ppm of the surfactant. This could be explained by the formation of the hydrogen bonding between the hydrogen of the hydroxyl group of the CSNs in the aqueous phase and the negatively charged oxygen present at the head of the surfactant molecules, resulting in the reduction of free surfactant molecules of SDS present in the aqueous solution, which contributes to the

https://doi.org/10.1021/acsomega.1c00296
ACS Omega 2021, 6, 11327−11339

adsorption (Figure 4).[20,34,45] However, there could be many possible reasons that may be responsible for the surfactant adsorption reduction in the presence of nanoparticles. The addition of CSNs could shield the sand surface, resulting in hindering the interaction of the surfactant and the sand surface. The surfactant molecules would now interact with the CSNs only, resulting in a lower adsorption of the surfactant.[29] Another possible explanation for the surfactant adsorption reduction could be the competitive adsorption of the CSNs on the sand surface. This would result in limiting the adsorption sites available for the surfactant, resulting in a lower adsorption of the surfactant. Also, the CSNs and the surfactant could form negatively charged clusters that would reside in the bulk phase, keeping the surfactant molecules away from the rock surface, resulting in a lower surfactant adsorption.[46] However, if the nanoparticles were not present in the aqueous phase, all the free surfactant molecules present in the solution were readily available for adsorption; hence, higher adsorption values were obtained in such cases (Figure 5).

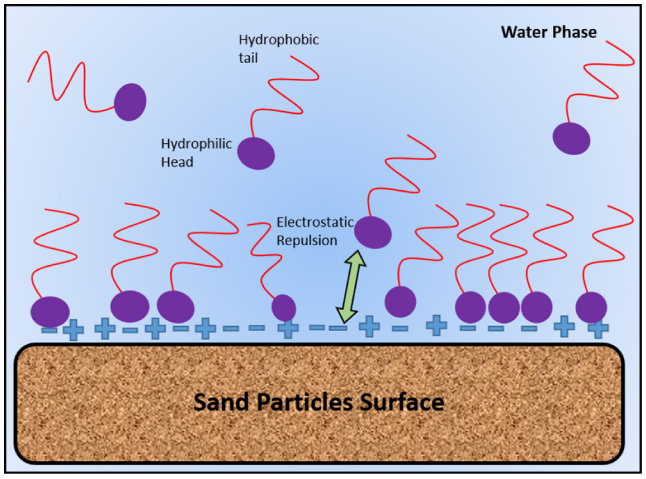

Figure 5. Adsorption of SDS on the sand particle surface in the absence of CSNs.

The increase in the nanoparticle concentration also affected the CMC value of the surfactant. The CMC of the surfactant was found to be reduced from 2483 ppm (8.61 mM) to 2164 ppm (7.50 mM) as the concentration of the CSNs in the solution was increased from 0 to 25 vol %, respectively (Figure 6). This could be attributed to the increase in the ionic strength of the solution. Since CSNs are small in size and would have a higher surface charge density, it would promote the dissociation of the ions in the solution. This could lead to a decrease in the electrostatic repulsive force between the surfactant molecules, forcing the surfactant to form micelles even at a lower concentration.[47,48] The reduction in the CMC of the surfactant could be attributed to an increase in the ionic concentration in the solution in the presence of nanoparticles that would promote the micellization of the surfactant even at a lower concentration.[49,50] Similar results were obtained in the present study, and the presence of CSNs would have increased the ionic strength of the surfactant solution; as a result, the micellization of the surfactant appeared even at lower concentrations.

3.2.1. Surfactant Adsorption in the Presence of Polymer and CSNs. A fixed quantity of the conventional industrial polymer PAM (1000 ppm) was mixed with the solution to

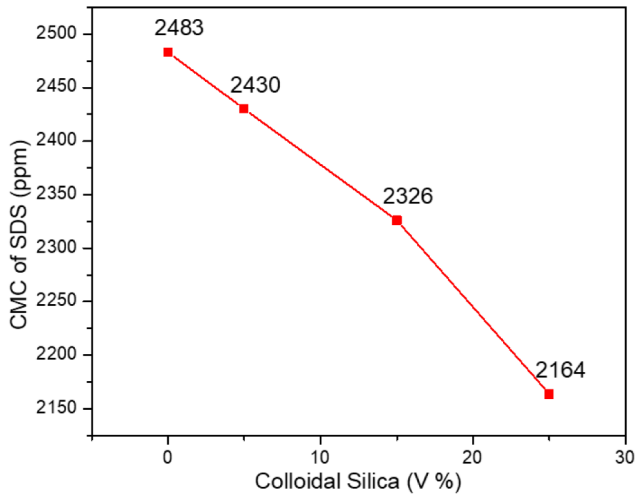

Figure 6. Effect of CSNs on the CMC of the surfactant.

check its effect on the adsorption of the surfactant in the presence of CSNs. The concentration of the surfactant as well as the CSNs was varied. The addition of a polymer reduced the adsorption of the surfactant, as reported in previous studies.[51] The adsorption of SDS with 25 vol % CSNs reduced from 0.974 to 0.894 mg/g when a polymer was added to the solution at 2500 ppm of the surfactant. This could be attributed to the adsorption of polymer on the sand particle surface, leaving lesser adsorption sites for surfactant adsorption.[52,53] Another possible explanation for the surfactant adsorption reduction in the presence of the polymer could be the reduction of repulsion between the surfactant molecules because of the steric hindrance offered by the large polymer chains.[22,54] The presence of a polymer could also result in the adsorption of a few surfactant molecules on their surface keeping them in the bulk phase rather than interacting with the sand surface. Also, the presence of a long polymeric chain could hinder the interaction of free surfactant molecules and the rock surface that could result in adsorption reduction. The effect of CSNs on the adsorption of the surfactant (Figure 7a), as well as the effect of surfactant concentration on the reduction of adsorption percentage (Figure 7b), remained the same as that without a polymer.

3.2.2. Comparison in the Reduction Percentage of the Adsorption of Surfactant. Figure 8 shows the comparison in the reduction of the adsorption percentage of the surfactant on the sand particle surface at different concentrations of the surfactant and CSNs. The reduction percentage of the adsorption of the surfactant kept increasing when the concentration of the surfactant was below 2500 ppm. This is because the number of free molecules of the surfactant in the solution kept increasing till 2500 ppm, whereas afterward the adsorption of the surfactant did not change significantly; hence, the percentage reduction in adsorption also did not increase. The presence of the polymer also increased the reduction of adsorption. At 500 ppm of the surfactant with 5 vol % of CSNs, the reduction of adsorption was 17%, which increased to 21% upon the introduction of the polymer in the solution. This could be due to the steric hindrance offered by the larger and bulky molecules of polymers present in the solution.[13]

3.2.3. Effect of Time on Surfactant Adsorption. The adsorption of the surfactant on the sand particles with respect

https://doi.org/10.1021/acsomega.1c00296
ACS Omega 2021, 6, 11327−11339

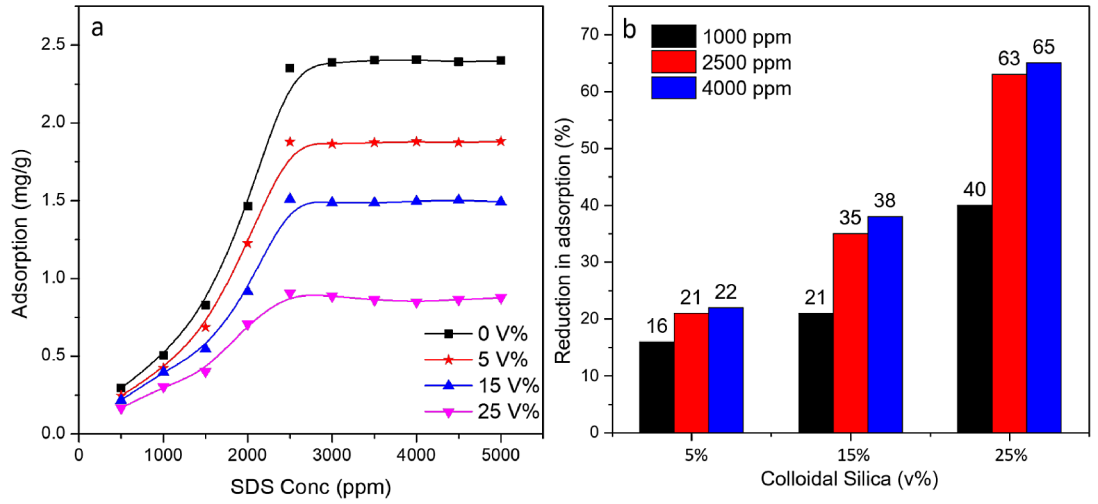

Figure 7. Surfactant adsorption in the presence of polymer. (a) Effect of CSNs on the reduction of surfactant adsorption. (b) Effect of surfactant concentration on the percentage reduction of adsorption.

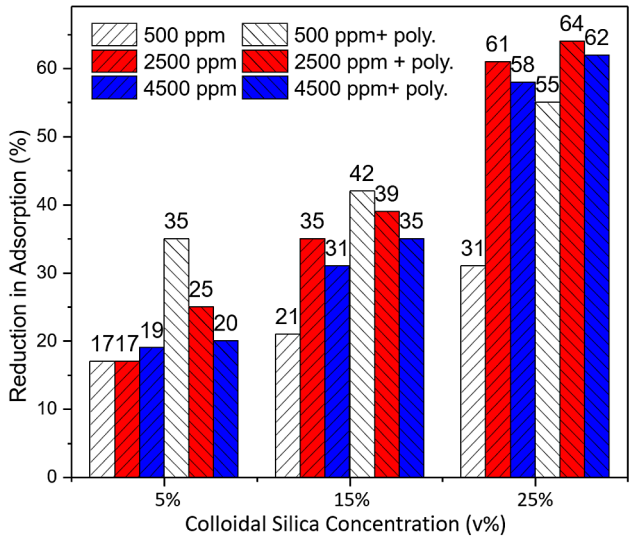

Figure 8. Comparison in the adsorption reduction percentage in the presence and absence of polymer with variation in CSN concentration at different concentrations of the surfactant.

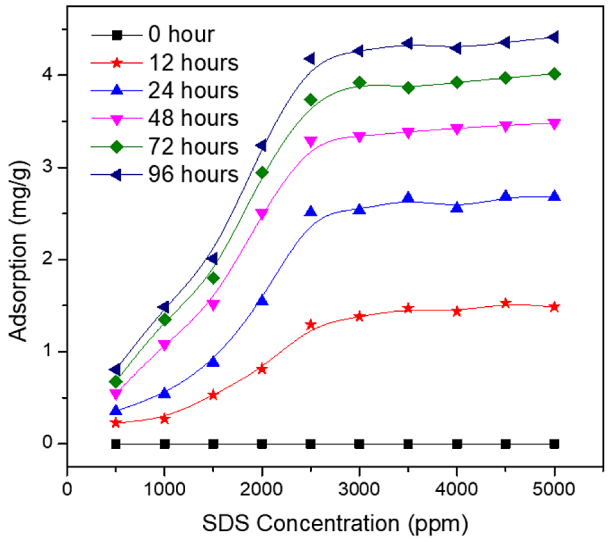

Figure 9. Effect of time on the adsorption of the surfactant.

to time was also measured, and the results showed that the adsorption of the surfactant increased with an increase in the time (Figure 9). The adsorption of the surfactant was measured with variation in the surfactant concentration as well as with variation in time. It was found that the surfactant adsorption follows the Langmuir isotherm (Figure 10). The Langmuir isotherm was plotted using eq 2.[35,44,55−57]

$$Q_e = \frac{Q_o K_{ad} C_e}{1 + K_{ad} C_e} \quad (2)$$

where Q_e and Q_o are the equilibrium adsorption (mg/g rock) and adsorption capacity in the Langmuir model (mg/g rock), C_e is the equilibrium concentration, and K_{ad} is the Langmuir adsorption constant.

The value of the standard Gibbs free energy related to the adsorption of the surfactant on the sand surface was calculated using eq 3.[58]

$$\Delta G^0 = -RT \ln K_L \quad (3)$$

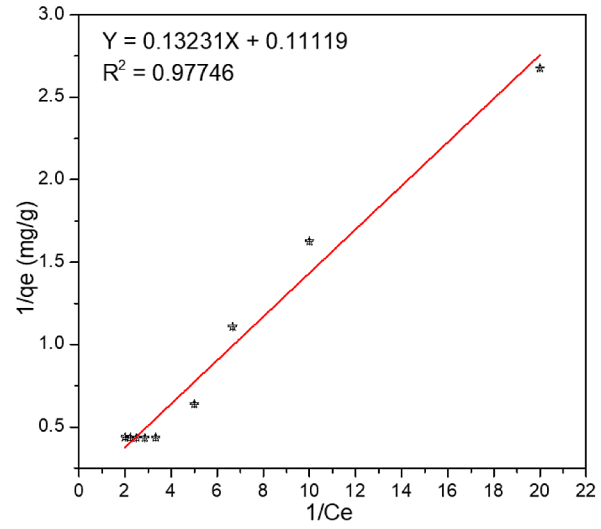

Figure 10. Langmuir adsorption model.

https://doi.org/10.1021/acsomega.1c00296
ACS Omega 2021, 6, 11327−11339

where K_L is the thermodynamic equilibrium constant and is obtained as $K_L = Q_o K_{ad}$, R is the universal gas constant (8.314 J/mol K), and T is the temperature (K). The ΔG value for the adsorption of the surfactant on sand particles was found to be −5095.22 J/mol at 30 °C. The negative value suggests the spontaneous nature of the adsorption.[58]

3.3. Surface Tension and Wettability Studies. Surface tension is one of the most crucial parameters that affect oil recovery. The lesser the surface tension, the easier it is for the displacing fluid to displace the crude oil from the pore spaces, which would result in higher oil recovery. Hence, it becomes essential to measure the surface tension of the slug, which is to be injected into the sand pack. It was found that the surface tension with water was 71.5 mN/m, which decreased to 49.2 mN/m when the 2500 ppm surfactant and 1000 ppm polymer were added to the water at 25 °C. In another study, the surface tension of pure water was reported to be 71.41 mN/m.[42] A similar trend in the reduction of the surface tension value of SDS was obtained in past studies.[59] The surface tension value reduced to 40.8 mN/m upon the addition of the 25 vol % CSNs to the solution (Figure 11). This could be attributed to the adsorption of the nanoparticles at the interface of the air/liquid and thereby reduced IFT.[31,32,60−63] The reduction in the IFT value is highly desirable in the case of surfactant flooding. The lower IFT or surface tension value suggested that it would be easier for the displacing fluid to displace the oil present in the pore spaces of the rock, which implies that more oil could be recovered from the core leaving lesser residual oil saturation behind. These results are consistent with the previous findings.[64]

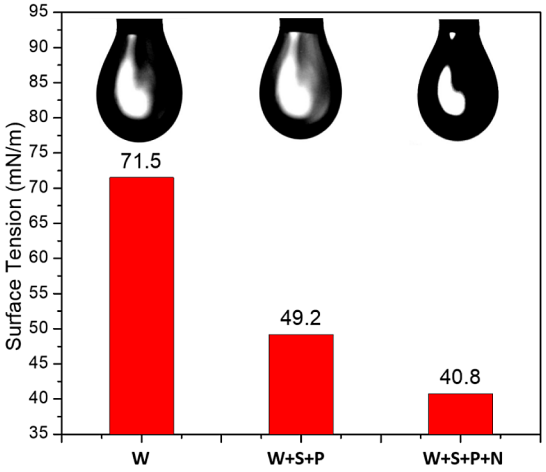

Figure 11. Surface tension measurement of water (W); water, surfactant (S), and polymer (P); and water, surfactant, polymer, and CSNs (N).

Another important parameter that affects the oil recovery directly is the wettability alteration capability of the slug, which was investigated by the contact angle measurement. Sessile drop experiments were performed to find out the effect of CSNs on the alteration of the wettability.[65] It was found that the contact angle reduced when the surfactant and polymer were added to the solution and then decreased further upon the addition of nanoparticles to the solution. The contact angle was measured at a different time interval, and it was found to be decreasing with time (Figure 12). The contact angle in the case of distilled water was found to be 100° after 10 s when the drop was placed on the glass slide covered with oil film, whereas the contact angle of the drop containing 2500 ppm surfactant and 1000 ppm polymer was found to be 88° at the same time, which reduced to a value of 51° at 600 s. The decrease in contact angle indicates the effect of the surfactant on the reduction of IFT and shifting of the wettability toward water-wet. The decrease in the contact angle could be due to the adsorption of the surfactant on the surface.[11,66] On the addition of 25 vol % CSNs to the solution, the contact angle further reduced to a value of 82°, which further decreased to a minimum value of 43° at 600 s. The reduction of the contact angle in the presence of nanoparticles could be attributed to the adsorption of nanoparticles on the interface.[67,68] The reduction in the contact angle clearly indicates the shifting of wettability from mixed wetting toward water-wet.

3.4. Viscosimetry Analysis. The flow behavior of the solution containing the surfactant and polymer is affected by the presence of nanoparticles. To truly understand the flow behavior of these mixtures, rheological studies are of utmost importance. The size, shape, and concentration of nanoparticles affect the rheology of the fluid.[69−71] Therefore, the viscosity of the fluid containing CSNs of varying concentrations was analyzed. The viscosity of the fluid was monitored over a wide range of shear rates. It was found that the viscosity of the fluid containing 2500 ppm of the surfactant and 1000 ppm of PAM reduced from 0.32 Pa s to a value of 0.005 Pa s upon the variation of the shear rate from 1 to 1000 s^{-1}. This showed the shear-thinning property of the fluid, which was also observed in the previous studies conducted by Meyer et al.[72] As the CSNs were introduced in the chemical slug, the improvement in the viscosity was observed. The addition of

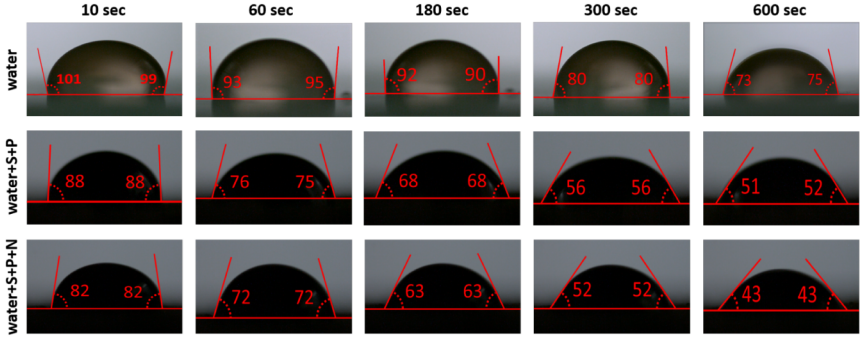

Figure 12. Contact angle measurement of water (W); water, surfactant (S), and polymer (P); water, surfactant polymer, and CSNs (N) with respect to time.

https://doi.org/10.1021/acsomega.1c00296
ACS Omega 2021, 6, 11327−11339

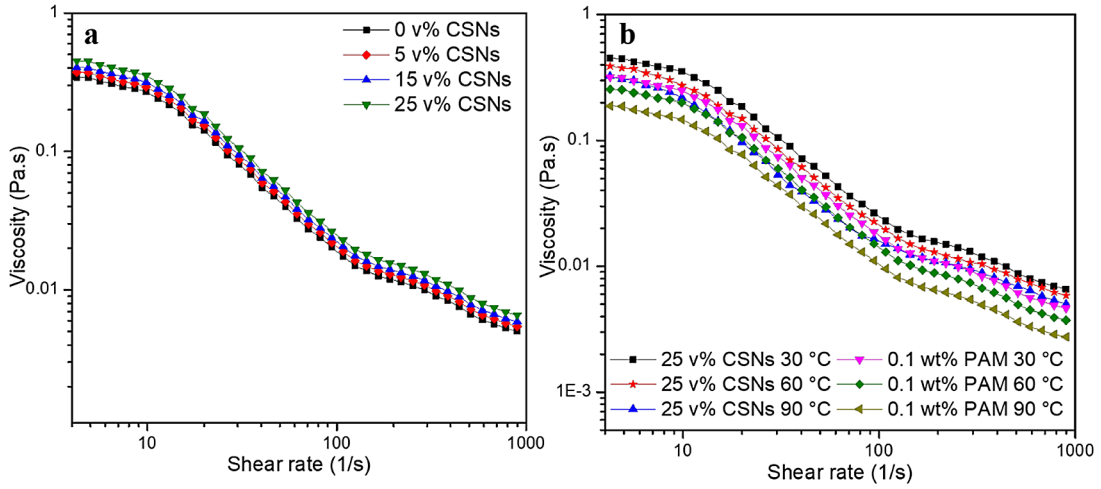

Figure 13. Viscosity: (a) effect of CSN concentration in the chemical slug; (b) effect of temperature on chemical slug composed of (i) PAM and the surfactant and (ii) PAM, surfactant, and CSNs.

nanoparticles increased the viscosity of the fluid from 0.32 Pa s (0 vol %) to 0.37 Pa s (5 vol %), 0.41 Pa s (15 vol %), and 0.45 Pa s (25 vol %) at 4.24 s^{-1} shear rate (Figure 13a); the results are in line with the findings of Mahbubul et al.[70] This could be attributed to the increase in the concentration of the solid particles present in the fluid. Another explanation for the improvement in the viscosity with CSNs is the formation of the complex molecular structure with the polymer chain that gave rise to the viscosity values. The increase in the viscosity would lead to a decrease in the mobility ratio and therefore would reduce the viscous fingering, as a result of which more oil would be swept achieving a higher volumetric sweep efficiency.[73]

As the temperature was increased from 30 to 60 °C and 90 °C, the viscosity of the slug (25 vol % CSNs + 1000 ppm polymer + 2500 ppm surfactant) was found to decrease (Figure 13b). The viscosity reduced from 0.45 Pa s (30 °C) to 0.39 Pa s and 0.32 Pa s at 60 and 90 °C, respectively, at 4.24 s^{-1} shear rate. The reduction in the viscosity of nanofluids, when compared with PAM solution, was less. The viscosity reduction of the 25 vol % CSNs was 13.7% (0.45−0.39 Pa s) and 28.2% (0.45−0.32 Pa s), whereas the same for PAM solution was 19.7% (0.32−0.26 Pa s) and 41% (0.32−0.19 Pa s) at 60 and 90 °C, when compared with the viscosity at 30 °C at 4.24 s^{-1} shear rate. The reduction in the viscosity of the polymeric fluid could be attributed to an increase in the kinetic energy of the polymer molecules when heated, as a result of which the weak entanglement between the polymer chains could break, giving rise to a decrease in the viscosity of the PAM when the temperature was increased.[11,74] However, the addition of CSNs decreased the reduction in the viscosity of the polymeric fluid. This could be attributed to the formation of a complex macromolecular structure between the CSNs and the polymer chain. The results are consistent with the previous studies.[72,75]

To verify the experimental results of the chemical slug showing shear-thinning behavior, modeling analysis was performed. Since the experimental results showed the shear-thinning property, which is the property of the non-Newtonian fluid, Ostwald−de Waele (commonly known as power-law model) was fitted using the experimental data of the chemical slug (PAM 1000 ppm, surfactant at 2500 ppm, and 25 vol % CSNs) using the eq 4.[76,77] The flow behavior index and the consistency index of the chemical slug were analyzed by fitting the experimentally measured values of the shear stress and shear rate in the power-law model. The results of the modeling analysis are given in Table 1. The regression correlation coefficient (R^2) values approaching 1, validating the shear-thinning flow behavior of the chemical slug obtained via experimental values. The value of $n \in (0.55-0.62)$ suggested that the chemical slug was pseudoplastic.[78] With variation in the temperature, the value of n has a little change but still falls in the pseudoplastic region.

Table 1. Power-Law Modeling Analysis

s. no	temperature (°C)	n (flow behavior index)	K (consistency index)	R^2
1	30	0.55143	0.131	0.99764
2	60	0.63765	0.073	0.99937
3	90	0.61993	0.064	0.99740

$$\tau = K\gamma^n \quad (4)$$

where τ is the shear stress (Pa), K is the consistency index, γ is the shear rate (s^{-1}), and n is the flow behavior index.

3.5. Particle Size Distribution and Zeta Potential. The size of the particles to be added to the chemical slug has a great impact on the interfacial property, as a result of which oil recovery would be affected; hence, it becomes critical to investigate the particle size of the CSNs added to the chemical slug. The results obtained show that only one peak was found, indicating that CSNs were not agglomerated, which is highly desirable in the case of nanoparticles to work efficiently. The average hydrodynamic diameter of the CSNs was found to be 20.34 nm (Figure 14), which is smaller than the pore throat sizes of the rock. Now, smaller size CSNs would be able to intrude into the pore throats of the rocks and get adsorbed on the water oil interface, resulting in the reduction of the IFT between the fluids.[73] The reduction in the IFT would result in the reduction of the capillary pressure acting on the oil drops at the pore throat, which would make it easier for the displacing fluid to displace the oil from such smaller pores. The smaller size of the CSNs would also have more electrostatic repulsion between the nanoparticles and the liquid (water + surfactant + polymer solution), which would give rise to the

https://doi.org/10.1021/acsomega.1c00296
ACS Omega 2021, 6, 11327−11339

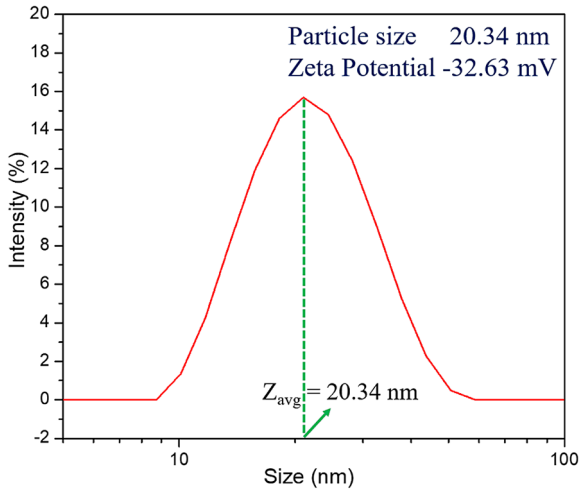

Figure 14. Particle size and zeta potential of the CSNs.

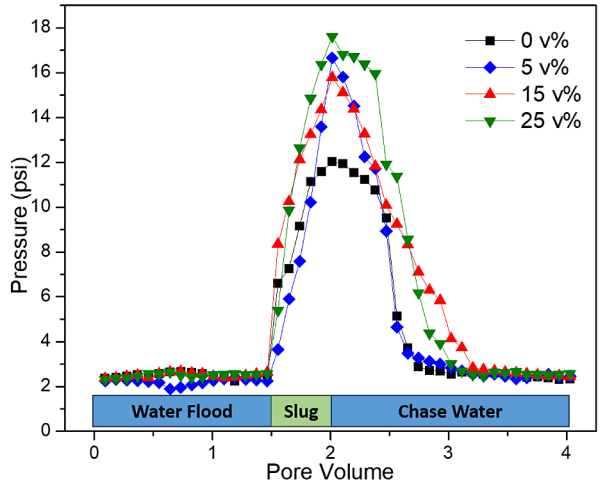

Figure 15. Pressure drop obtained with a variation in the CSN concentration.

adsorption of nanoparticles on the surface, leading to the reduction in the surface tension.[79] This was evident in the surface tension and contact angle measurement Section 3.5), where the addition of CSNs reduced the surface tension of the chemical slug and also shifted the wettability toward water-wet. The addition of silica nanoparticles has been previously used to alter the wettability of the rock toward water-wet.[80] Moreover, smaller size nanoparticles have a larger surface energy per unit area as a result of which effectively reduces the surface tension as well as shifts the wettability toward water-wet.[73,81] Apart from the effect of nanoparticle size on the surface tension and wettability, viscosity is another important parameter that gets affected. The addition of smaller nanoparticles also increases the viscosity of the fluid.[71] An increase in the viscosity of the displacing fluid would lead to a decrease in the mobility ratio.[73] This would increase the macroscopic displacement efficiency. The combined effect of the addition of smaller size CSNs on the reduction of the IFT, wettability alteration, and increasing the viscosity of the displacing fluid would be able to recover more oil.

The zeta potential of the CSNs dispersed in deionized water was determined to obtain their stability. The zeta potential of the CSNs dispersed in water was found to be −32.63 mV (average of three measurements) that falls in the range beyond ±30 mV, which is the range of the zeta potential indicating the electrophoretic stability of the particles dispersed in a liquid.[82] The agglomeration of the particles starts when the value of the zeta potential lies in the range of ±15 mV, whereas the sample will precipitate out if the zeta potential is zero.[82,83] The negative zeta potential could be due to the hydroxyl group of the silica present in the CSNs.

3.6. Flooding Experiments. The pressure drop is defined as the difference in the pressure obtained between the inlet and outlet of the sand pack during the flooding process. It indicates the flow of the fluid inside the sand pack. The pressure drop obtained during the surfactant polymer flooding was found to increase as the injected fluid was changed from water to chemical slug (Figure 15). A sudden increase in the pressure drop was found at 1.5 PV, which is due to the high viscosity of the injected fluid. The pressure drop was continued to increase from 2.39 to 12.03 psi because of the increase in the viscosity of the injection fluid from 0.001 Pa s (water) to 0.007 Pa s (chemical slug with 25 vol % CSNs) at 1000 s^{-1} shear rate, after which it started reducing again because of the change in the viscosity of the injected fluid and stabilized around the value of ∼2.4 psi due to the reduction in the viscosity of the injection fluid (chemical slug to chase water). As the concentration of CSNs in the chemical slug was varied, the pressure drop shows a little increment that could be attributed to the presence of more viscous fluid (CSNs) in the chemical slug, which could be verified by the increase in the viscosity of the fluid observed in the viscosity results of the fluids (Section 3.4).

The oil recovery with waterflood was found to be ∼48%, whereas an additional recovery of 23% of OOIP (original oil in place) was found when the surfactant polymer slug was flooded, followed by the chase water (Table 2). As the CSN concentration was varied in the chemical slug, the oil recovery was found to be increasing (Figure 16). The secondary recovery remains the same, ∼48%, whereas an additional recovery or tertiary recovery was increased from 23% to 28%. This could be attributed to the presence of nanoparticles that would have been able to reduce the surfactant adsorption, which would have increased the surfactant activity and hence increased the ultimate oil recovery.[6] Another reason for the increase in oil recovery could be the reduction of surface tension as well the shifting of wettability toward water-wet as the CSNs were introduced in the chemical slug, which is supported by the surface tension and contact angle results. The increase in CSNs in the chemical slug increased the ultimate oil recovery. The water cut is the fraction of the produced fluid which is water. It is used as an indication of the completion of the flooding process. As the water cut reached 100%, oil production ceased and the flooding was stopped. The water cut reached ∼100% from 1 to 1.5 PV, which explains the injection of the chemical slug at 1.5 PV, whereas a sudden fall in water cut after 2 PV could be attributed to the time taken by the chemical slug front to move from the injection end of the sand pack to the outlet. A sudden decrease in water cut reflects the increase in oil recovery, which justifies the oil recovery curve. The increase in water cut again reflects the production of the chase water, which pushes the oil bank behind the chemical slug front.

https://doi.org/10.1021/acsomega.1c00296
ACS Omega 2021, 6, 11327−11339

Table 2. Parameters Obtained While Flooding

run no.	Φ (%)	K (mD) K_w $S_w = 1$	K_o S_{oi}	chemical slug composition	saturation (%) S_{wi}	S_{oi}	S_{va}	oil recovery (% OOIP) secondary	additional oil	cumulative
1	34.46	544	320	0.5 PV (1000 ppm PAM + 2500 ppm surfactant)	19.55	80.45	28.74	48.13	23.13	71.26
2	34.72	606	326	0.5 PV (1000 ppm PAM + 2500 ppm surfactant + 5 vol % CSNs)	19.03	80.97	27.42	46.65	25.93	72.58
3	35.37	589	276	0.5 PV (1000 ppm PAM + 2500 ppm surfactant + 15 vol % CSNs)	21.62	78.38	26.07	46.49	27.45	73.94
4	35.13	561	299	0.5 PV (1000 ppm PAM + 2500 ppm surfactant + 25 vol % CSNs)	20.87	79.13	24.28	47.22	28.82	76.04

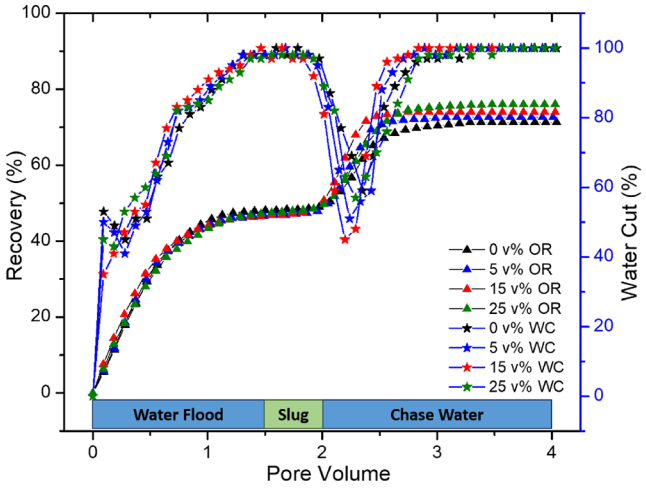

Figure 16. Oil recovery and water cut with the variation of CSN concentration.

4. CONCLUSIONS

The application of 25 vol % CSNs effectively reduced the adsorption of the 2500 ppm surfactant on the sand particles surface up to 61% in the absence of polymer, which increased to 64% in the presence of 1000 ppm polymer at 2500 ppm of the surfactant. The CMC of the surfactant was found to be dependent on the CSN concentration present in the fluid. The CMC of the surfactant reduced from 2483 ppm in the absence of CSNs to 2164 ppm with 25 vol % of CSNs in the solution. CSNs also affected the surface tension as well as the wettability characteristics. The surface tension value of water at 25 °C was found to be 71.5 mN/m, which reduced to a value of 49.2 mN/m upon the introduction of 2500 ppm surfactant and 1000 ppm polymer. The addition of 25 vol % CSNs further reduced the surface tension values of 40.8 mN/m. The contact angle was found to be 73° in the case of water at 600 s, which reduced to a value of 51° upon the introduction of 2500 ppm surfactant and 1000 ppm polymer. The addition of CSNs further reduced the contact angle to a value 43°, shifting the wettability toward water-wet effectively. The rheological property of the chemical slug was also found to be improved with the CSNs. The viscosity of the slug improved from 0.32 to 0.45 Pa s at 4.24 s^{-1} shear rate with 25 vol % of CSNs at 30 °C. The reduction in the adsorption of the surfactant, as well as improvement in the viscosity of the slug, was reflected as the improved oil recovery results. The addition of 25 vol % CSNs in the surfactant polymer flooding achieved an additional recovery of up to 5% when compared to the conventional surfactant polymer flooding. Hence, CSNs could be used effectively for EOR.

AUTHOR INFORMATION

Corresponding Authors

Shivanjali Sharma − *Department of Petroleum Engineering and Geological Sciences, Rajiv Gandhi Institute of Petroleum Technology, Jais 229304, India;* orcid.org/0000-0002-6212-8267; Email: ssharma@rgipt.ac.in

Ajay Mandal − *Department of Petroleum Engineering Indian Institute of Technology (ISM), Enhanced Oil Recovery Laboratory, Dhanbad 826004, India;* orcid.org/0000-0003-2947-4261; Email: ajay@iitism.ac.in

Author

Himanshu Kesarwani − *Department of Petroleum Engineering and Geological Sciences, Rajiv Gandhi Institute of Petroleum Technology, Jais 229304, India*

Complete contact information is available at: https://pubs.acs.org/10.1021/acsomega.1c00296

Notes

The authors declare no competing financial interest.

ACKNOWLEDGMENTS

This work has been funded by the Rajiv Gandhi Institute of Petroleum Technology, Jais, India.

REFERENCES

(1) Gbadamosi, A. O.; Junin, R.; Manan, M. A.; Augustine, A.; Oseh, J. O.; Usman, J. Synergistic Application of Aluminium Oxide Nanoparticles and Oilfield Polyacrylamide for Enhanced Oil Recovery. *J. Pet. Sci. Eng.* **2019**, *182*, No. 106345.

(2) Shamsijazeyi, H.; Miller, C. A.; Wong, M. S.; Tour, J. M.; Verduzco, R. Polymer-Coated Nanoparticles for Enhanced Oil Recovery. *J. Appl. Polym. Sci.* **2014**, *131*, 1−13.

(3) Pogaku, R.; Fuat, N. H. M.; Sakar, S.; Cha, Z. W.; Musa, N.; Tajudin, D. N. A. A.; Morris, L. O. Polymer Flooding and Its Combinations with Other Chemical Injection Methods in Enhanced Oil Recovery. *Polym. Bull.* **2018**, *75*, 1753−1774.

(4) Gbadamosi, A. O.; Junin, R.; Manan, M. A.; Yekeen, N.; Agi, A.; Oseh, J. O. Recent Advances and Prospects in Polymeric Nanofluids Application for Enhanced Oil Recovery. *J. Ind. Eng. Chem.* **2018**, *66*, 1−19.

(5) Pillai, P.; Kumar, A.; Mandal, A. Mechanistic Studies of Enhanced Oil Recovery by Imidazolium-Based Ionic Liquids as Novel Surfactants. *J. Ind. Eng. Chem.* **2018**, *63*, 262−274.

(6) Zargartalebi, M.; Kharrat, R.; Barati, N. Enhancement of Surfactant Flooding Performance by the Use of Silica Nanoparticles. *Fuel* **2015**, *143*, 21−27.

(7) Spildo, K.; Sun, L.; Djurhuus, K.; Skauge, A. A. Strategy for Low Cost, Effective Surfactant Injection. *J. Pet. Sci. Eng.* **2014**, *117*, 8−14.

(8) Lu, J.; Goudarzi, A.; Chen, P.; Kim, D. H.; Delshad, M.; Mohanty, K. K.; Sepehrnoori, K.; Weerasooriya, U. P.; Pope, G. A. Enhanced Oil Recovery from High-Temperature, High-Salinity

Naturally Fractured Carbonate Reservoirs by Surfactant Flood. *J. Pet. Sci. Eng.* **2014**, *124*, 122−131.
(9) Ponce, F. R. V.; Carvalho, M. S.; Alvarado, V. Oil Recovery Modeling of Macro-Emulsion Flooding at Low Capillary Number. *J. Pet. Sci. Eng.* **2014**, *119*, 112−122.
(10) Druetta, P.; Raffa, P.; Picchioni, F. Chemical Enhanced Oil Recovery and the Role of Chemical Product Design. *Appl. Energy* **2019**, *252*, No. 113480.
(11) Kumar, S.; Saxena, N.; Mandal, A. Synthesis and Evaluation of Physicochemical Properties of Anionic Polymeric Surfactant Derived from Jatropha Oil for Application in Enhanced Oil Recovery. *J. Ind. Eng. Chem.* **2016**, *43*, 106−116.
(12) Gbadamosi, A. O.; Junin, R.; Manan, M. A.; Yekeen, N.; Augustine, A. Hybrid Suspension of Polymer and Nanoparticles for Enhanced Oil Recovery. *Polym. Bull.* **2019**, *76*, 6193−6230.
(13) Deepatana, A.; Valix, M. Steric Hindrance Effect on Adsorption of Metal-Organic Complexes onto Aminophosphonate Chelating Resin. *Desalination* **2008**, *218*, 297−303.
(14) Co, L.; Zhang, Z.; Ma, Q.; Watts, G.; Zhao, L.; Shuler, P. J.; Tang, Y. Evaluation of Functionalized Polymeric Surfactants for EOR Applications in the Illinois Basin. *J. Pet. Sci. Eng.* **2015**, *134*, 167−175.
(15) Pal, N.; Saxena, N.; Divya Laxmi, K. V.; Mandal, A. Interfacial Behaviour, Wettability Alteration and Emulsification Characteristics of a Novel Surfactant: Implications for Enhanced Oil Recovery. *Chem. Eng. Sci.* **2018**, *187*, 200−212.
(16) Aitkulov, A.; Mohanty, K. K. Investigation of Alkaline-Surfactant-Polymer Flooding in a Quarter Five-Spot Sandpack for Viscous Oil Recovery. *J. Pet. Sci. Eng.* **2019**, *175*, 706−718.
(17) Kumar, S.; Mandal, A. Rheological Properties and Performance Evaluation of Synthesized Anionic Polymeric Surfactant for Its Application in Enhanced Oil Recovery. *Polymer (Guildf)* **2017**, *120*, 30−42.
(18) Kurnia, I.; Zhang, G.; Han, X.; Yu, J. Zwitterionic-Anionic Surfactant Mixture for Chemical Enhanced Oil Recovery without Alkali. *Fuel* **2020**, *259*, No. 116236.
(19) Seethepalli, A.; Adibhatla, B.; Mohanty, K. K. Physicochemical Interactions during Surfactant Flooding of Fractured Carbonate Reservoirs. *SPE J.* **2004**, *9*, 411−418.
(20) Saxena, N.; Kumar, A.; Mandal, A. Adsorption Analysis of Natural Anionic Surfactant for Enhanced Oil Recovery: The Role of Mineralogy, Salinity, Alkalinity and Nanoparticles. *J. Pet. Sci. Eng.* **2019**, *173*, 1264−1283.
(21) Wang, J.; Han, M.; Fuseni, A. B.; Cao, D. Surfactant Adsorption in Surfactant-Polymer Flooding for Carbonate Reservoirs. *SPE Middle East Oil Gas Show Conf. MEOS, Proc.* **2015**, *2015-Janua*, 1736−1746.
(22) Pal, N.; Kumar, N.; Mandal, A. Stabilization of Dispersed Oil Droplets in Nanoemulsions by Synergistic Effects of the Gemini Surfactant, PHPA Polymer, and Silica Nanoparticle. *Langmuir* **2019**, *35*, 2655−2667.
(23) Munshi, A. M.; Singh, V. N.; Kumar, M.; Singh, J. P. Effect of Nanoparticle Size on Sessile Droplet Contact Angle. *J. Appl. Phys.* **2008**, *103*, 10−15.
(24) Chaturvedi, K. R.; Trivedi, J.; Sharma, T. Single-Step Silica Nanofluid for Improved Carbon Dioxide Flow and Reduced Formation Damage in Porous Media for Carbon Utilization. *Energy* **2020**, *197*, No. 117276.
(25) Chaturvedi, K. R.; Kumar, R.; Trivedi, J.; Sheng, J. J.; Sharma, T. Stable Silica Nanofluids of an Oilfield Polymer for Enhanced CO2 Absorption for Oilfield Applications. *Energy and Fuels* **2018**, *32*, 12730−12741.
(26) Sharma, T.; Iglauer, S.; Sangwai, J. S. Silica Nanofluids in an Oilfield Polymer Polyacrylamide: Interfacial Properties, Wettability Alteration, and Applications for Chemical Enhanced Oil Recovery. *Ind. Eng. Chem. Res.* **2016**, *55*, 12387−12397.
(27) Zargartalebi, M.; Barati, N.; Kharrat, R. Influences of Hydrophilic and Hydrophobic Silica Nanoparticles on Anionic Surfactant Properties: Interfacial and Adsorption Behaviors. *J. Pet. Sci. Eng.* **2014**, *119*, 36−43.
(28) Almahfood, M.; Bai, B. The Synergistic Effects of Nanoparticle-Surfactant Nanofluids in EOR Applications. *J. Pet. Sci. Eng.* **2018**, *171*, 196−210.
(29) Wu, Y.; Chen, W.; Dai, C.; Huang, Y.; Li, H.; Zhao, M.; He, L.; Jiao, B. Reducing Surfactant Adsorption on Rock by Silica Nanoparticles for Enhanced Oil Recovery. *J. Pet. Sci. Eng.* **2017**, *153*, 283−287.
(30) Yekeen, N.; Padmanabhan, E.; Idris, A. K. Synergistic Effects of Nanoparticles and Surfactants on N-Decane-Water Interfacial Tension and Bulk Foam Stability at High Temperature. *J. Pet. Sci. Eng.* **2019**, *179*, 814−830.
(31) Saien, J.; Bahrami, M. Understanding the Effect of Different Size Silica Nanoparticles and SDS Surfactant Mixtures on Interfacial Tension of N-Hexane−Water. *J. Mol. Liq.* **2016**, *224*, 158−164.
(32) Cheraghian, G.; Hendraningrat, L. A. Review on Applications of Nanotechnology in the Enhanced Oil Recovery Part A: Effects of Nanoparticles on Interfacial Tension. *Int. Nano Lett.* **2016**, *6*, 129−138.
(33) Ahmadi, M. A.; Sheng, J. Performance Improvement of Ionic Surfactant Flooding in Carbonate Rock Samples by Use of Nanoparticles. *Pet. Sci.* **2016**, *13*, 725−736.
(34) Zhuang, G. L.; Tseng, H. H.; Wey, M. Y. Preparation of PPO-Silica Mixed Matrix Membranes by in-Situ Sol-Gel Method for H2/CO2 Separation. *Int. J. Hydrogen Energy* **2014**, *39*, 17178−17190.
(35) Ahmadi, M. A.; Shadizadeh, S. R. Induced Effect of Adding Nano Silica on Adsorption of a Natural Surfactant onto Sandstone Rock: Experimental and Theoretical Study. *J. Pet. Sci. Eng.* **2013**, *112*, 239−247.
(36) Ahmadi, M. A.; Shadizadeh, S. R. Nano-Surfactant Flooding in Carbonate Reservoirs: A Mechanistic Study. *Eur. Phys. J. Plus* **2017**, *132*, No. 246.
(37) Ahmadi, M. A. Use of Nanoparticles to Improve the Performance of Sodium Dodecyl Sulfate Flooding in a Sandstone Reservoir. *Eur. Phys. J. Plus* **2016**, *131*, No. 435.
(38) Khan, M. Y.; Samanta, A.; Ojha, K.; Mandal, A. Interaction between Aqueous Solutions of Polymer and Surfactant and Its Effect on Physicochemical Properties. *Asia-Pac. J. Chem. Eng.* **2008**, *3*, 579−585.
(39) Ahmadi, M. A.; Shadizadeh, S. R. Adsorption of Novel Nonionic Surfactant and Particles Mixture in Carbonates: Enhanced Oil Recovery Implication. *Energy and Fuels* **2012**, *26*, 4655−4663.
(40) Rahimi, K.; Adibifard, M. Experimental Study of the Nanoparticles Effect on Surfactant Absorption and Oil Recovery in One of the Iranian Oil Reservoirs. *Pet. Sci. Technol.* **2015**, *33*, 79−85.
(41) Kesarwani, H.; Saxena, A.; Mandal, A.; Sharma, S. Anionic/Nonionic Surfactant Mixture for Enhanced Oil Recovery through the Investigation of Adsorption, Interfacial, Rheological, and Rock Wetting Characteristics. *Energy & Fuels* **2021**, *35*, 3065−3078.
(42) Wolowicz, A.; Staszak, K. Study of Surface Properties of Aqueous Solutions of Sodium Dodecyl Sulfate in the Presence of Hydrochloric Acid and Heavy Metal Ions. *J. Mol. Liq.* **2020**, *299*, No. 112170.
(43) Marcolongo, J. P.; Mirenda, M. Thermodynamics of Sodium Dodecyl Sulfate (SDS) Micellization: An Undergraduate Laboratory Experiment. *J. Chem. Educ.* **2011**, *88*, 629−633.
(44) Ahmadi, M. A.; Shadizadeh, S. Experimental and Theoretical Study of a New Plant Derived Surfactant Adsorption on Quartz Surface: Kinetic and Isotherm Methods. *J. Dispersion Sci. Technol.* **2015**, *36*, 441−452.
(45) Setiawan, W. K.; Chiang, K. Y. Silica Applied as Mixed Matrix Membrane Inorganic Filler for Gas Separation: A Review. *Sustainable Environ. Res.* **2019**, *1*, 1−21.
(46) Yekeen, N.; Manan, M. A.; Idris, A. K.; Samin, A. M.; Risal, A. R. Experimental Investigation of Minimization in Surfactant Adsorption and Improvement in Surfactant-Foam Stability in Presence of Silicon Dioxide and Aluminum Oxide Nanoparticles. *J. Pet. Sci. Eng.* **2017**, *159*, 115−134.
(47) Eftekhari, M.; Schwarzenberger, K.; Javadi, A.; Eckert, K. The Influence of Negatively Charged Silica Nanoparticles on the Surface

https://doi.org/10.1021/acsomega.1c00296
ACS Omega 2021, 6, 11327−11339

Properties of Anionic Surfactants: Electrostatic Repulsion or the Effect of Ionic Strength? *Phys. Chem. Chem. Phys.* **2020**, *22*, 2238−2248.
(48) Palladino, P.; Ragone, R. Ionic Strength Effects on the Critical Micellar Concentration of Ionic and Nonionic Surfactants: The Binding Model. *Langmuir* **2011**, *27*, 14065−14070.
(49) Tanford, C. The Hydrophobic Effect: Formation of Micelles and Biological Membranes (2nd Edition). *Biochem. Soc. Trans.* **1981**, *9*, 178.
(50) Umlong, I. M.; Ismail, K. Micellization of AOT in Aqueous Sodium Chloride, Sodium Acetate, Sodium Propionate, and Sodium Butyrate Media: A Case of Two Different Concentration Regions of Counterion Binding. *J. Colloid Interface Sci.* **2005**, *291*, 529−536.
(51) Sjöberg, M.; Bergström, L.; Larsson, A.; Sjöström, E. The Effect of Polymer and Surfactant Adsorption on the Colloidal Stability and Rheology of Kaolin Dispersions. *Colloids Surf., A* **1999**, *159*, 197−208.
(52) Cheraghian, G.; Nezhad, S. S. K.; Kamari, M.; Hemmati, M.; Masihi, M.; Bazgir, S. Adsorption Polymer on Reservoir Rock and Role of the Nanoparticles, Clay and SiO 2. *Int. Nano Lett.* **2014**, *4*, 114.
(53) Sadowski, Z.; Polowczyk, I. Effect of Polymer-Surfactant Adsorption on the Hindered Settling of a Mineral Suspension. *Adsorpt. Sci. Technol.* **2001**, *19*, 245−254.
(54) Lv, W.; Zhou, Z.; Zhang, Q.; Luo, W.; Wang, H.; Ma, D.-S.; Zhang, L.; Wang, R.; Zhang, L. Soft Matter Wetting of Polymer Surfaces by Aqueous Solutions of Branched Cationic Gemini Surfactants. *Soft Matter* **2019**, *15*, 6725−6731.
(55) Ahmadi, M. A.; Shadizadeh, S. R. Spotlight on the New Natural Surfactant Flooding in Carbonate Rock Samples in Low Salinity Condition. *Sci. Rep.* **2018**, *8*, No. 10985.
(56) Kazemzadeh, Y.; Sharifi, M.; Riazi, M.; Rezvani, H.; Tabaei, M. Potential Effects of Metal Oxide/SiO2 Nanocomposites in EOR Processes at Different Pressures. *Colloids Surf., A* **2018**, *559*, 372−384.
(57) Liu, Z.; Hedayati, P.; Sudhölter, E. J. R.; Haaring, R.; Shaik, A. R.; Kumar, N. Adsorption Behavior of Anionic Surfactants to Silica Surfaces in the Presence of Calcium Ion and Polystyrene Sulfonate. *Colloids Surf., A* **2020**, *602*, No. 125074.
(58) Chiban, M.; Carja, G.; Lehutu, G.; Sinan, F. Equilibrium and Thermodynamic Studies for the Removal of As(V) Ions from Aqueous Solution Using Dried Plants as Adsorbents. *Arab. J. Chem.* **2016**, *9*, S988−S999.
(59) Hernáinz, F.; Caro, A. Variation of Surface Tension in Aqueous Solutions of Sodium Dodecyl Sulfate in the Flotation Bath. *Colloids Surf., A* **2002**, *196*, 19−24.
(60) Pal, N.; Verma, A.; Ojha, K.; Mandal, A. Nanoparticle-Modified Gemini Surfactant Foams as Efficient Displacing Fluids for Enhanced Oil Recovery. *J. Mol. Liq.* **2020**, *310*, No. 113193.
(61) Kumar, A.; Mandal, A. Critical Investigation of Zwitterionic Surfactant for Enhanced Oil Recovery from Both Sandstone and Carbonate Reservoirs: Adsorption, Wettability Alteration and Imbibition Studies. *Chem. Eng. Sci.* **2019**, *209*, No. 115222.
(62) Pal, N.; Vajpayee, M.; Mandal, A. Cationic/Nonionic Mixed Surfactants as Enhanced Oil Recovery Fluids: Influence of Mixed Micellization and Polymer Association on Interfacial, Rheological, and Rock-Wetting Characteristics. *Energy and Fuels* **2019**, *33*, 6048−6059.
(63) Pillai, P.; Mandal, A. A Comprehensive Micro Scale Study of Poly-Ionic Liquid for Application in Enhanced Oil Recovery: Synthesis, Characterization and Evaluation of Physicochemical Properties. *J. Mol. Liq.* **2020**, *302*, No. 112553.
(64) Ma, T.; Feng, H.; Wu, H.; Li, Z.; Jiang, J.; Xu, D.; Meng, Z.; Kang, W. Property Evaluation of Synthesized Anionic-Nonionic Gemini Surfactants for Chemical Enhanced Oil Recovery. *Colloids Surf., A* **2019**, *581*, No. 123800.
(65) Pillai, P.; Mandal, A. Wettability Modification and Adsorption Characteristics of Imidazole-Based Ionic Liquid on Carbonate Rock: Implications for Enhanced Oil Recovery. *Energy and Fuels* **2019**, *33*, 727−738.
(66) Zdziennicka, A.; Jańczuk, B. The Relationship between the Adhesion Work, the Wettability and Composition of the Surface Layer in the Systems Polymer/Aqueous Solution of Anionic Surfactants and Alcohol Mixtures. *Appl. Surf. Sci.* **2010**, *257*, 1034−1042.
(67) Cheraghian, G.; Rostami, S.; Afrand, M. Nanotechnology in Enhanced Oil Recovery. *Processes* **2020**, *8*, 1−17.
(68) Bera, A.; Shah, S.; Shah, M.; Agarwal, J.; Vij, R. K. Mechanistic Study on Silica Nanoparticles-Assisted Guar Gum Polymer Flooding for Enhanced Oil Recovery in Sandstone Reservoirs. *Colloids Surf., A* **2020**, *598*, No. 124833.
(69) Kumar, R. S.; Sharma, T. Stability and Rheological Properties of Nanofluids Stabilized by SiO2 Nanoparticles and SiO2-TiO2 Nanocomposites for Oilfield Applications. *Colloids Surf., A* **2018**, *539*, 171−183.
(70) Mahbubul, I. M.; Saidur, R.; Amalina, M. A. Latest Developments on the Viscosity of Nanofluids. *Int. J. Heat Mass Transf.* **2012**, *55*, 874−885.
(71) Lu, W. Q.; Fan, Q. M. Study for the Particle's Scale Effect on Some Thermophysical Properties of Nanofluids by a Simplified Molecular Dynamics Method. *Eng. Anal. Bound. Elem.* **2008**, *32*, 282−289.
(72) Meyer, J. P.; Adio, S. A.; Sharifpur, M.; Nwosu, P. N. The Viscosity of Nanofluids: A Review of the Theoretical, Empirical, and Numerical Models. *Heat Transfer Eng.* **2016**, *37*, 387−421.
(73) Rezk, M. Y.; Allam, N. K. Impact of Nanotechnology on Enhanced Oil Recovery: A Mini-Review. *Ind. Eng. Chem. Res.* **2019**, *58*, 16287−16295.
(74) Hashmet, M. R.; Onur, M.; Tan, I. M. Empirical Correlations for Viscosity of Polyacrylamide Solutions with the Effects of Temperature and Shear Rate. II. *J. Dispersion Sci. Technol.* **2014**, *35*, 1685−1690.
(75) Yang, Y.; Zhang, Z. G.; Grulke, E. A.; Anderson, W. B.; Wu, G. Heat Transfer Properties of Nanoparticle-in-Fluid Dispersions (Nanofluids) in Laminar Flow. *Int. J. Heat Mass Transf.* **2005**, *48*, 1107−1116.
(76) Hasan, S. W.; Ghannam, M. T.; Esmail, N. Heavy Crude Oil Viscosity Reduction and Rheology for Pipeline Transportation. *Fuel* **2010**, *89*, 1095−1100.
(77) Ariffin, T. S. T.; Yahya, E.; Husin, H. The Rheology of Light Crude Oil and Water-in-Oil-Emulsion. *Procedia Eng.* **2016**, *148*, 1149−1155.
(78) Sheng, J. J. Polymer Flooding-Fundamentals and Field Cases. In *Enhanced Oil Recovery Field Case Studies*; Elsevier Inc., 2013; pp. 63−82. DOI: DOI: 10.1016/B978-0-12-386545-8.00003-8
(79) Brown, M. A.; Duyckaerts, N.; Redondo, A. B.; Jordan, I.; Nolting, F.; Kleibert, A.; Ammann, M.; Wörner, H. J.; Van Bokhoven, J. A.; Abbas, Z. Effect of Surface Charge Density on the Affinity of Oxide Nanoparticles for the Vapor-Water Interface. *Langmuir* **2013**, *29*, 5023−5029.
(80) Hendraningrat, L.; Torsæter, O. Effects of the Initial Rock Wettability on Silica-Based Nanofluid-Enhanced Oil Recovery Processes at Reservoir Temperatures. *Energy and Fuels* **2014**, *28*, 6228−6241.
(81) Bhuiyan, M. H. U.; Saidur, R.; Amalina, M. A.; Mostafizur, R. M.; Islam, A. K. M. S. Effect of Nanoparticles Concentration and Their Sizes on Surface Tension of Nanofluids. *Procedia Eng.* **2015**, *105*, 431−437.
(82) Salopek, B.; Krasić, D.; Filipović, S. Measurement and Application of Zeta Potential. *Rud. Zb.* **1992**, *4*, 147−151.
(83) Lu, G. W.; Gao, P. Emulsions and Microemulsions for Topical and Transdermal Drug Delivery. In *Handbook of Non-Invasive Drug Delivery Systems*; Elsevier, 2010; pp. 59−94. DOI: DOI: 10.1016/B978-0-8155-2025-2.10003-4

https://doi.org/10.1021/acsomega.1c00296
ACS Omega 2021, 6, 11327−11339